

# High Performance Wide Angle DBR Design for Optoelectronic Devices

Volume 13, Number 1, February 2021

Ting Zhi

Tao Tao

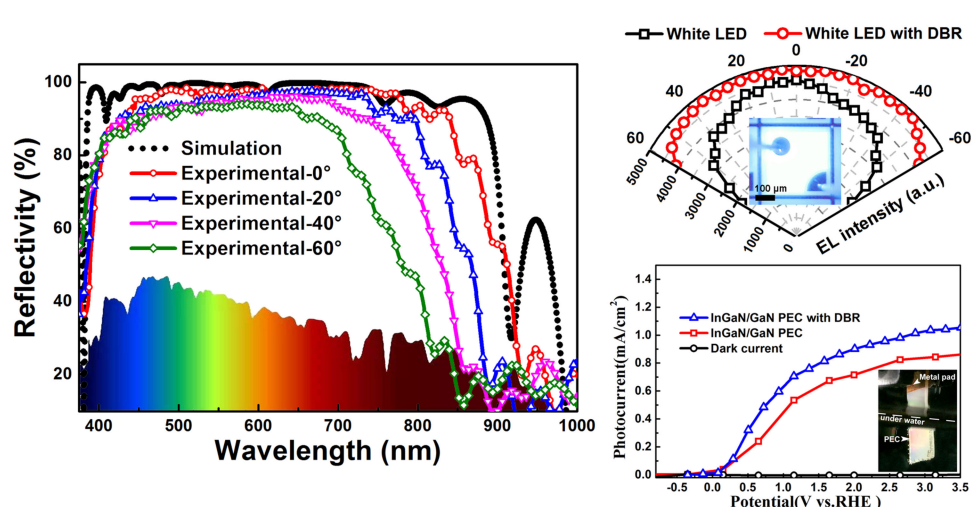
Bin Liu, *Member, IEEE*

Yan Yu

Zili Xie

Hong Zhao

Dunjun Chen, *Member, IEEE*



DOI: 10.1109/JPHOT.2021.3050761

# High Performance Wide Angle DBR Design for Optoelectronic Devices

Ting Zhi,<sup>1</sup> Tao Tao ,<sup>2</sup> Bin Liu ,<sup>2</sup> Member, IEEE, Yan Yu,<sup>2</sup> Zili Xie,<sup>2</sup> Hong Zhao,<sup>2</sup> and Dunjun Chen,<sup>2</sup> Member, IEEE

<sup>1</sup>College of Electronic and Optical Engineering and College of Microelectronics, Nanjing University of Posts and Telecommunications, Nanjing 210093, China

<sup>2</sup>Jiangsu Provincial Key Laboratory of Advanced Photonic and Electronic Materials, School of Electronic Science and Engineering, Nanjing University, Nanjing 210093, China

DOI:10.1109/JPHOT.2021.3050761

This work is licensed under a Creative Commons Attribution 4.0 License. For more information, see <https://creativecommons.org/licenses/by/4.0/>

Manuscript received September 11, 2020; revised December 29, 2020; accepted January 6, 2021. Date of publication January 11, 2021; date of current version January 28, 2021. This work was supported in part by the National Nature Science Foundation of China under Grants 62004104 and 61974062, in part by the Nature Science Foundation of Jiangsu Province under Grants BK20180747 and BE2015111, in part by National Key Research and Development Program of China under Grant 2017YFB0404101, in part by Collaborative Innovation Center of Solid State Lighting and Energy-saving Electronics, and in part by Open Fund of the State Key Laboratory on Integrated Optoelectronics under Grant IOSKL2017KF03. Corresponding author: Tao Tao (e-mail: ttao@nju.edu.cn).

**Abstract:** To improve the performance of optoelectronic devices, a high performance wide angle  $\text{SiO}_2/\text{Ti}_3\text{O}_5$  Distributed Bragg Reflector (DBR) mirror was designed and fabricated on double polished sapphire substrate. 17-pairs gradually varied DBR structure was applied in order to acquire a broad stopband reflectivity over 95% from 400 nm to 800 nm, covering the whole visible light region. The DBR mirrors deposited at the backside of optoelectronics devices are also demonstrated to remain a high reflectivity at wide incident angles, which improves the emission efficiency of LEDs and light absorption efficiency of InGaN/GaN photoelectrochemical cell (PEC).

**Index Terms:** Distributed Bragg Reflector (DBR) mirror,  $\text{SiO}_2/\text{Ti}_3\text{O}_5$ , light emitting diodes, PEC.

## 1. Introduction

III-Nitride solid-state light emitters are attracting increasing attentions due to their wide applications ranging from light communication [1], high resolution display [2], [3], energy harvest [4] and lasers [5], [6]. For instance, the conventional approach is to mainly use InGaN/GaN-based blue light emitting diodes with color conversion phosphor materials, such as  $\text{Y}_3\text{Al}_5\text{O}_{12}:\text{Ge}^{3+}$ (YAG), to generate artificial white light [7], [8]. Despite many works have been devoted to the development of white LED during the past decade, current GaN-based white LEDs are still mainly grown on sapphire substrate due to the consideration of lattice matching and coefficient of thermal expansion in the growth process [9], [10]. Light lost emitting through the transparent sapphire substrate is still a key problem that influences the emission efficiency [11]. Thus the backside mirror with high reflectivity in visible light region are still needed for improving the efficiency of GaN-based LEDs and solar energy harvest devices [12]–[14].

The DBR based on  $\text{SiO}_2/\text{SiN}_x/\text{Ti}_3\text{O}_5$  film can provide high reflectivity because of relative large contrast of refractive index between  $\text{SiO}_2$  and  $\text{SiN}_x/\text{Ti}_3\text{O}_5$  [15]. On the other hand, DBR films can be

Table 1  
Deposition Parameters of  $\text{SiO}_2$  and  $\text{SiN}_x$  Layers By PECVD

Growth parameters	$\text{SiO}_2$	$\text{SiN}_x$
Chamber temperature/°C	350	350
RF power/W	10	50
Chamber pressure/mTorr	300	500
$\text{SiH}_4/\text{N}_2$ gas flow/sccm	100	25
$\text{N}_2\text{O}$ gas flow/sccm	400	/
$\text{N}_2$ gas flow/sccm	/	400
$\text{NH}_3$ gas flow/sccm	/	20

deposited by PECVD/PVD directly on the backside of LEDs or photodetectors, hence giving higher structure/chemical stability and cost saving compared to the usage of high value Ag or Al metal layer [16]. However, it is very challenging to grow high quality DBR mirror with high reflectivity covering the whole visible light region. Normally, reflectivity in longer and shorter wavelength regions require two contradictory parameters that one needs thicker periodic layers to increase optical path difference and the other needs thinner layers because of the characteristics of DBR mirror [17]. Furthermore, reflectivity of DBR mirror will decrease dramatically with respect to the increasing incident angle due to the increase in optical path difference at higher incident angles.

In this work,  $\text{SiO}_2/\text{SiN}_x$  and  $\text{SiO}_2/\text{Ti}_3\text{O}_5$  DBR mirrors have been designed and fabricated to improve the reflectivity covering a wide visible light region and incident angle as well. The structure and growth parameters of DBR mirror were optimized by means of optical properties analysis and theoretical simulation. Finally, the optoelectronic performance, especially wide angle emission, of white LED with optimized backside DBR mirror were enhanced. In addition, the energy conversion efficiency of PEC was increased by integrating the DBR mirror to the backside of solar cell, which demonstrates the promising potentials for many optoelectronic applications including light emitting devices, photodetectors and solar cells.

## 2. Experimental

$\text{SiO}_2/\text{SiN}_x$  DBR mirrors were fabricated by plasma-enhanced chemical vapor deposition (OXFORD Plasma 80 Plus PECVD) on double-polished sapphire substrates. While,  $\text{SiO}_2/\text{Ti}_3\text{O}_5$  DBR mirrors were grown by physic vapor deposition (KJLC, PVD75), where the growth rate were controlled by the electron beam power. In this work, the silicon precursors were  $\text{SiH}_4/\text{N}_2$  (5%). The temperature of growth chamber were controlled to be 350°. The growth parameters for  $\text{SiO}_2$ ,  $\text{SiN}_x$  and  $\text{Ti}_3\text{O}_5$  films were optimized to acquire smooth and clear interface, details can be seen in Table 1. The growth rate are determined by the deposition speed calculated by the measured thickness of each layer using a step profiler and a broadband spectroscopic ellipsometer (EOPTICS ME-L). And optical constants about refractive index ( $n$ ) and extinction coefficient ( $k$ ) were simulated by anslysis software, which can be found in our previous report [18].

In addition, all the backside DBR mirrors were fabricated according to the theoretical simulation by software TFCalculator. The reflectivity spectra of all samples were measured by UV-visible spectrometer (SHIMADZU UV-3600). The surface morphologies of samples were obtained by atomic force microscope (ND-MDT Modular AFM).

## 3. Results and Discussion

As illustrated by the schematic diagram of a traditional single main-function unit DBR structure in Fig. 1(a), 27 pairs of  $\text{SiO}_2/\text{SiN}_x$  layers (83.75 nm/59.96 nm) can provide high reflectivity region close

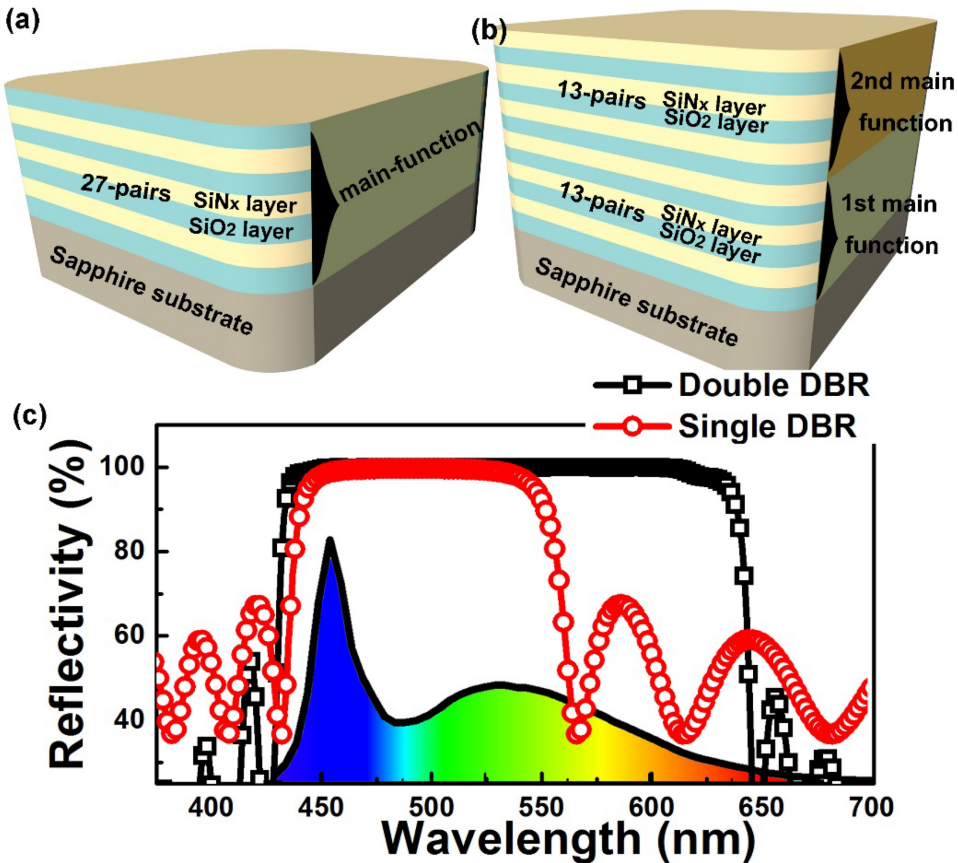


Fig. 1. (a) Schematic diagram of traditional single main-function unit periodic DBR; (b) Schematic diagram of double main-function units periodic DBR; and (c) Simulated reflectivity spectra of single/double DBR structures.

to 99% as shown in Fig. 1(c)(red line), only a center wavelength of 490 nm and a narrow stopband width of 90 nm from 450 nm to 550 nm can be seen. Normally, the radiation efficiency of blue LED has reached as much as 70%, while the color conversed yellow and red emission still need improvement. The single periodic DBR can cover the emission region of blue and green LEDs, leaving the yellow and red region unchanged. In other words, thicker color conversion phosphor materials are needed in order to provide enough yellow emission.

For the sake of providing high reflectivity covering the white LED emission region, a combination of multi mirrors with wide stopband from 400 nm to 700 nm are expected. According to this requirement, the structure of backside DBR were optimized by using the transfer matrix method based on the experimental optical constants of SiO<sub>2</sub> and SiN<sub>x</sub>, respectively. The optimized DBR mirror consists of a double periodic main-function units as illustrated in Fig. 1(b). The thickness of SiO<sub>2</sub> layer (SiN<sub>x</sub> layer) in first main-function unit are 97.86 nm (69.64 nm), and those in second main-function unit are 82.20/58.5 nm, respectively. The thickness of SiO<sub>2</sub> and SiN<sub>x</sub> layers are calculated by  $d = \lambda_0 / 4n$ , which are key elements determining the high reflectivity center and stopband [19]. As shown by the simulated reflectivity spectra of the SiO<sub>2</sub>/SiN<sub>x</sub> periodic DBRs in Fig. 1(c)(black line), the double main-function units DBR design could expand the stopband width to a wider 200 nm from 440 nm to 650 nm. It can be seen that double units DBR can provide high reflectivity within both of the blue and yellow emission region.

As demonstrated by actual reflectivity of double units DBR sample in Fig. 2(red line), the experimental reflectivity spectrum of optimized DBR mirror sample is in a good coincidence with

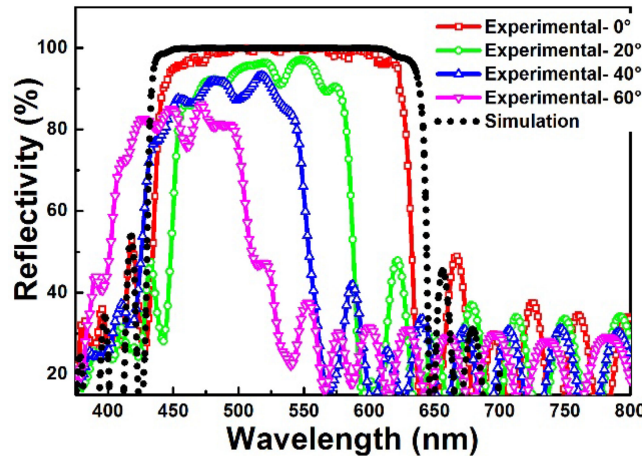


Fig. 2. Experimental reflectivity spectra of double units  $\text{SiO}_2/\text{SiN}_x$  DBR samples with respect to the incident angle.

the simulated spectrum (black dot line). The stopband width of actual reflectivity is slightly smaller than simulation, which might be attributed to the H-atom related defects, rough interface and the formation of thin Si-O-N transition layer between  $\text{SiO}_2$  and  $\text{SiN}_x$  layers. The Si-O-N transition layer with graded composition, has been widely reported in other references, can have major effects on the discrepancy in reflectivity near the edge of stopband [17].

On the other hand, the center wavelength of DBR sample exhibit obvious blue-shift with respect to the increasing light incident angle, as shown in Fig. 2. Meantime, the maximum reflectivity decrease and the stopband width are reduced as well, which is mainly because of the changed optical path difference at higher incident angles. It is hard to ignore such degradation in reflectivity with respect to incident angles, especially in current LED devices which are mostly grown on patterned sapphire substrate. It should be mentioned that the reflectivity of DBR might approach 100%, when the incident angle of light is larger than the total internal reflection angle at the sapphire/ $\text{SiO}_2$  interface, since the DBR mirror was deposited on the backside of sapphire.

In order to settle problems above,  $\text{Ti}_3\text{O}_5$  layer was applied to replace the  $\text{SiN}_x$  layer because of its higher refractive index ( $\sim 2.35$ ). The larger difference of refractive index ( $n$ ) between two materials could reduce the number of periodicity required for high reflectivity. And the formation of Si-O-N transition layer could be suppressed during the deposition process, giving improved interface. Furthermore, 17-pairs gradually varied DBR structure was designed as shown in Fig. 3(a) in order to remain high reflectivity at wide incident angles.

It can be seen that the experimental reflectivity spectra of  $\text{SiO}_2/\text{Ti}_3\text{O}_5$  periodic DBRs are in a good coincidence with the reflectivity spectra simulated with the use of TFCalculator, which can provide a much wider stopband from 400 nm to 850 nm. As illustrated by the color solar radiation spectrum, the high reflectivity stopband of  $\text{SiO}_2/\text{Ti}_3\text{O}_5$  periodic DBRs can cover the whole visible light region, which might pave the way for wide applications in solar power harvest. It should be mentioned that the center wavelength of  $\text{SiO}_2/\text{Ti}_3\text{O}_5$  periodic DBR sample also exhibit a blue-shift with respect to the increasing light incident angle. But as shown by the experimental reflectivity spectra measured at  $60^\circ$  incident angle in Fig. 3(b)(green line), the  $\text{SiO}_2/\text{Ti}_3\text{O}_5$  periodic DBR still can give more than 90% reflectivity within the wavelength ranging from 400 nm to 700 nm. Therefore, it can be expected that such DBR mirror could provide improved performance of optoelectronic devices. Of course, the interface between each layer and the surface roughness need to be further improved in according to the cross sectional SEM and surface AFM images in Fig. 3(c) and (d).

To verify the actual effect of the DBR mirror,  $\text{SiO}_2/\text{Ti}_3\text{O}_5$  periodic DBR was deposited on the backside of a traditional white LED and InGaN/GaN PEC devices in this work. Angular distribution measurements of emission intensity ranging from  $-60^\circ$  to  $60^\circ$  have been conducted for LEDs

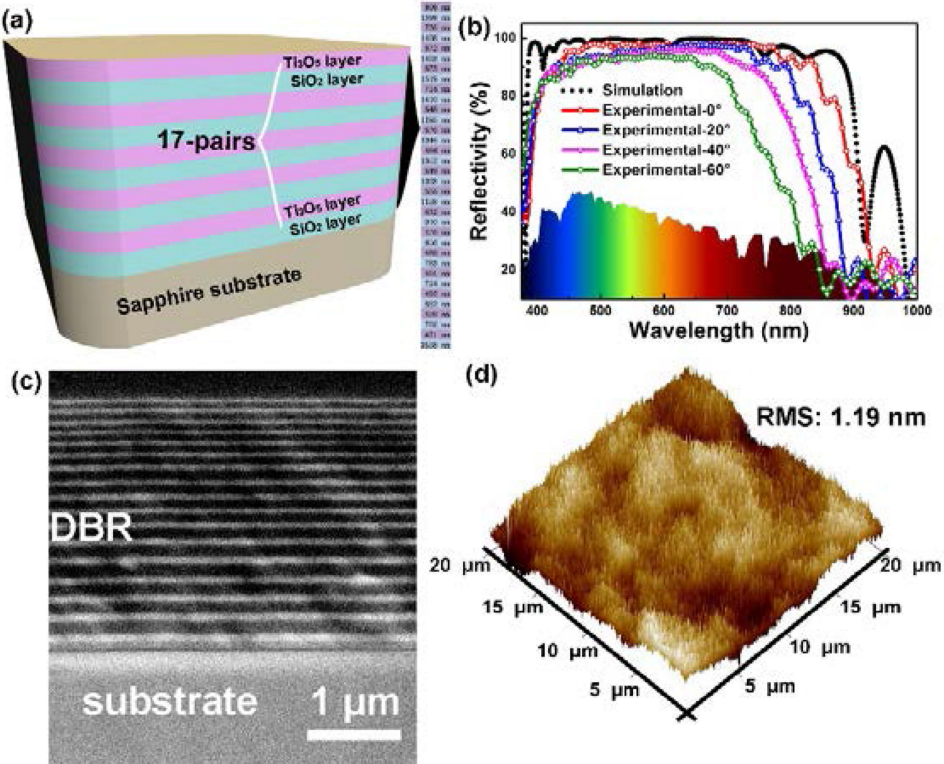


Fig. 3. (a) Schematic diagram of 17-pairs SiO<sub>2</sub>/Ti<sub>3</sub>O<sub>5</sub> DBR; (b) Experimental reflectivity spectra of SiO<sub>2</sub>/Ti<sub>3</sub>O<sub>5</sub> DBR samples with respect to the incident angle; (c) Cross sectional SEM image of 17-pairs SiO<sub>2</sub>/Ti<sub>3</sub>O<sub>5</sub> DBR; and (d) Surface AFM scanning image in 3D mode.

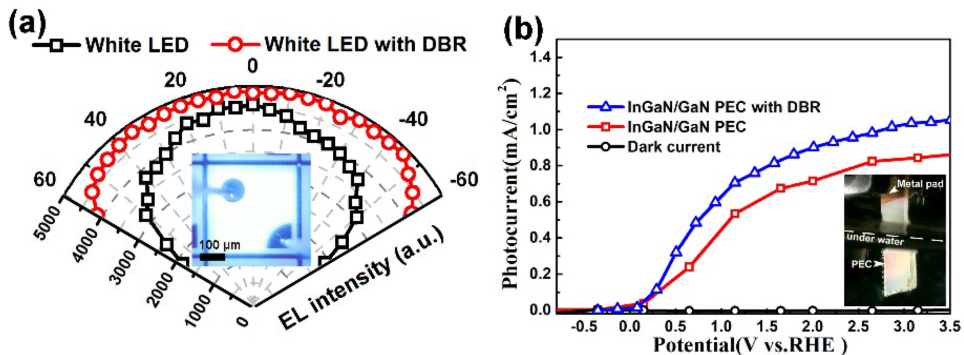


Fig. 4. (a) Angular distribution of LED with/without DBR from  $-60^\circ$  to  $60^\circ$ , Inset: traditional GaN-based white LED; and (b) Photocurrent of InGaN/GaN PECs with/without DBR, Inset: InGaN/GaN based PEC device.

with and without DBR. As illustrated in Fig. 4(a), the LED sample with DBR exhibit an enhanced emission intensity and a much more uniform spatial intensity distribution from  $-60^\circ$  to  $60^\circ$ , where the emission intensity of traditional LED deceases gradually with increasing incident angle. It can be conclude that DBR mirror at the backside of LED give a wider emission angle, where more light can be extracted within range of spatial azimuths, resulting in improved light extraction efficiency. On the other hand, the photocurrent of InGaN/GaN PEC, in other words hydrogen generation rate, are enhanced from  $0.8 \text{ mA/cm}^2$  to  $1 \text{ mA/cm}^2$  @3 V by adding DBR mirror at the backside as

demonstrated in Fig. 4(b). It can be seen that the absorption efficiency of PEC is improved by the backside DBR mirror, which demonstrates a promising way in the applications for solar energy harvest.

## 4. Conclusion

In summary, a high performance 17-pairs gradually varied  $\text{SiO}_2/\text{Ti}_3\text{O}_5$  DBR with stopband reflectivity over 95% from 400 nm to 800 nm has been designed and successfully fabricated. The  $\text{SiO}_2/\text{Ti}_3\text{O}_5$  periodic DBRs mirror can give more than 90% reflectivity within the visible light region even at high incident angles. The wide angle emission intensity of LED, absorption efficiency of PEC as well, can be significantly enhanced by integrating the  $\text{SiO}_2/\text{Ti}_3\text{O}_5$  DBR to the backside of substrate, which might pave the way for its wide applications in light emitting devices and solar power harvest.

*Competing Financial Interests:* The authors declare no competing financial interest.

---

## References

- [1] J. Cho, J. Hyuk Park, J. K. Kim, and E. Fred Schubert, "White light-emitting diodes: History, progress, and future," *Laser Photon. Rev.*, vol. 11, 2017, Art. no. 1600147.
- [2] T. Wu *et al.*, "Mini-Led and micro-led: Promising candidates for the next generation display technology," *Appl. Sci.-Basel*, vol. 8, no. 9, 2018, Art. no. 1557.
- [3] J. Zhao *et al.*, "Full-Color laser displays based on organic printed microlaser arrays," *Nat. Commun.*, vol. 10, no. 1, pp. 870.1–870.6, 2019.
- [4] C. R. Bowen, H. A. Kim, P. M. Weaver, and S. Dunn, "Piezoelectric and ferroelectric materials and structures for energy harvesting applications," *Energy Environ. Sci.*, vol. 7, no. 1, pp. 25–44, 2014.
- [5] S. I. Azzam *et al.*, "Ten years of spasers and plasmonic nanolasers," *Light: Sci. Appl.*, vol. 9, no. 1, pp. 90.1–90.21, 2020.
- [6] B. Liu *et al.*, "Hybrid light emitters and uv solar-blind avalanche photodiodes based on iii-nitride semiconductors," *Adv. Mater.*, 2019, Art. no. 1904354.
- [7] L. Su, X. Zhang, Y. Zhang, and A. L. Rogach, "Recent progress in quantum dot based white light-emitting devices," *Top. Curr. Chem.*, vol. 374, no. 4, pp. 25, 2016.
- [8] Z. Zhuang *et al.*, "High color rendering index hybrid III-Nitride/Nanocrystals white light-emitting diodes," *Adv. Funct. Mater.*, vol. 26, no. 1, pp. 36–43, 2016.
- [9] H. P. T. Nguyen *et al.*, "Breaking the carrier injection bottleneck of phosphor-free nanowire white light-emitting diodes," *Nano Lett.*, vol. 13, no. 11, pp. 5437–5442, 2013.
- [10] M. Djavid, H. P. T. Nguyen, S. Zhang, K. Cui, S. Fan, and Z. Mi, "Tunnel injection ingan/gan Dot-in-a-Wire white-light-emitting diodes," *Semicond. Sci. Technol.*, vol. 29, no. 8, 2014, Art. no. 085009.
- [11] S. F. Li and A. Waag, "Gan based nanorods for solid state lighting," *J. Appl. Phys.*, vol. 111, no. 7, 2012, Art. no. 071101.
- [12] S. Zhou, X. Liu, H. Yan, Z. Chen, Y. Liu, and S. Liu, "Highly efficient gan-based high-power flip-chip light-emitting diodes," *Opt. Exp.*, vol. 27, no. 12, pp. A669–A692, 2019.
- [13] S. Zhou *et al.*, "Numerical and experimental investigation of gan-based flip-chip light-emitting diodes with highly reflective ag/ti and ito/dbr ohmic contacts," *Opt. Exp.*, vol. 25, no. 22, pp. 26615–26627, 2017.
- [14] S. Zhou, C. Zheng, J. Lv, Y. Gao, R. Wang, and S. Liu, "Gan-Based flip-chip leds with highly reflective ito/dbr P-Type and via hole-based N-Type contacts for enhanced current spreading and light extraction," *Opt. Laser Technol.*, vol. 92, pp. 95–100, 2017.
- [15] L. Jian-Kai *et al.*, "Implementation of high-power gan-based leds with a textured 3-D backside reflector formed by inserting a self-assembled sio2 nanosphere monolayer," *IEEE Trans. Electron Devices*, vol. 61, no. 3, pp. 831–837, Mar. 2014.
- [16] T. Tao *et al.*, "Significant improvements in ingan/gan nano-photoelectrodes for hydrogen generation by structure and polarization optimization," *Sci. Rep.*, vol. 6, 2016, Art. no. 20218.
- [17] R. Yuan *et al.*, "A high-performance  $\text{SiO}_2/\text{SiN}_x$  1-D photonic crystal UV filter used for solar-blind photodetectors," *IEEE Photon. J.*, vol. 11, no. 4, pp. 1–7, Aug. 2019.
- [18] X. Liu *et al.*, "Numerical simulation and experimental investigation of gan-based flip-chip leds and top-emitting leds," *Appl. Opt.*, vol. 56, no. 34, pp. 9502–9509, 2017.
- [19] T.- H. Lin *et al.*, "Enhanced light emission in vertical-structured gan-based light-emitting diodes with trench etching and arrayed P-Electrodes," *Solid-State Electron.*, vol. 107, pp. 30–34, 2015.